The Carbon−Lithium Electron Pair Bond in $(CH_3Li)_n$ (n = 1, 2, 4)

F. Matthias Bickelhaupt,*[,†,‡] Nicolaas J. R. van Eikema Hommes,*[,†] Célia Fonseca Guerra,[§] and Evert Jan Baerends[§]

Computer-Chemie-Centrum, Institut für Organische Chemie, Universität Erlangen-Nürnberg, Nägelsbachstrasse 25, D-91052 Erlangen, Germany, and Afdeling Theoretische Chemie, Scheikundig Laboratorium der Vrije Universiteit, De Boelelaan 1083, NL-1081 HV Amsterdam, The Netherlands

Received December 18, 1995[⊗]

The monomer, dimer, and tetramer of methyllithium, $(CH_3Li)_n$ (n = 1, 2, 4), have been studied with use of density-functional (DFT) and conventional *ab initio* theory. The energy gain ΔE associated with the formation of $(CH_3-Li)_n$ from n Li• and n CH_3• radicals is −45.5, −132.7, and −308.6 kcal/mol for n = 1, 2, and 4 using nonlocal density-functionals and a large, doubly polarized triple-ζ STO basis (NL-SCF/TZ2P). The corresponding dimerization and tetramerization energies for methyllithium are −41.7 and −126.6 kcal/mol, respectively. The 298 K heat of formation of CH_3Li(g) is calculated to be 29.2 kcal/mol, using experimental ΔH_f values for CH_3•(g) and Li•(g). The low-energy lithium 2p orbitals are shown to play an active role in the bonding of the methyllithium aggregates and can be viewed as valence orbitals. A detailed analysis of the carbon−lithium bonding mechanism highlights the significant role of covalent contributions. In CH_3Li, we find a strongly polar C−Li electron pair bond in which charge is donated from Li 2s to the CH_3 $2a_1$ SOMO. The covalent character is indicated by 2s ± $2a_1$ mixing and a sizable lithium $2p_z$ participation. In $(CH_3-Li)_4$ the carbon−lithium bond is provided by two distinct orbital interactions: (1) an *essentially covalent* electron pair bond between the strongly sp hybridized Li−Li and C−C bonding fragment orbitals of the lithium cluster and the methyl cage, respectively, in A_1 symmetry; (2) a strongly polar electron pair bond between the corresponding triply degenerate Li−Li and C−C antibonding fragment orbital sets in T_2 symmetry. The situation is similar for $(CH_3Li)_2$. The electron density is analyzed using atomic charges from the following: (1) the natural population analysis (NPA); (2) the Hirshfeld method; (3) the Mulliken method as well as a modification which we term Modified Mulliken; (4) a scheme which we designate Voronoi deformation density (VDD); the VDD charges monitor the shift of electron density out of (Q > 0) or into (Q < 0) the Voronoi cell of an atom upon formation of the molecule from the isolated atoms. The degree of ionicity of the carbon−lithium bond decreases from ca. "50" down to "30%" along CH_3Li, $(CH_3Li)_2$, and $(CH_3Li)_4$, according to the Hirshfeld charges. This agrees with a similar trend emerging from the VDD charges as well as with the results of the electronic structure analysis. The NPA charges suggest that the carbon−lithium bond is ca. "90%" ionic and that the degree of ionicity is independent of the size of the aggregate.

1. Introduction

Modern *ab initio* quantum chemical studies have provided a largely ionic picture of the carbon−lithium bond (**1**).[1] Advanced population analysis methods, e.g.

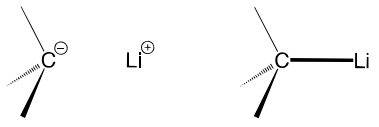

1 **2**

the natural population analysis (NPA) developed by Weinhold *et al.*,[2] as well as topological methods like Streitwieser's integrated projected population (IPP)[3a] or the atoms in molecules (AIM) approach due to Bader *et al.*[3b,c] yield lithium atomic charges between +0.75 and +0.90 e.[4,5] Thus, organolithium oligomers $(RLi)_n$ can be considered as aggregates of lithium cations and

† Universität Erlangen-Nürnberg.
‡ Present address: Baker Laboratory, Department of Chemistry, Cornell University, Ithaca, NY 14853-1301.
§ Vrije Universiteit.
⊗ Abstract published in *Advance ACS Abstracts,* June 1, 1996.

(1) (a) Streitwieser, A., Jr.; Bachrach, S. M.; Dorigo, A. E.; Schleyer, P. v. R. In *Lithium Chemistry*; Sapse, A. M., Schleyer, P. v. R., Eds.; J. Wiley and Sons: New York, 1995; Chapter 1 and references cited therein. (b) Lambert, C.; Schleyer, P. v. R. In *Carbanionen*. Methoden der Organischen Chemie (Houben-Weyl), Band E19d; Hanack, M., Ed.; Thieme: Stuttgart, Germany, 1993. (c) Lambert, C.; Schleyer, P. v. R. *Angew. Chem.* **1994**, *106*, 1187; *Angew. Chem., Int. Ed. Engl.* **1994**, *33*, 1129.

(2) (a) Reed, A. E.; Weinstock, R. B.; Weinhold, F. *J. Chem. Phys.* **1985**, *83*, 735. (b) Reed, A. E.; Curtiss, L. A.; Weinhold, F. *Chem. Rev.* **1988**, *88*, 899 and references cited therein. (c) Reed, A. E.; Schleyer, P. v. R. *J. Am. Chem. Soc.* **1990**, *112*, 1434.

(3) (a) Collins, J. B.; Streitwieser, A., Jr.; McKelvey, J. M. *J. Comput. Chem.* **1979**, *3*, 79. (b) Bader, R. W. F. *Acc. Chem. Res.* **1985**, *18*, 9. (c) Bader, R. W. F. *Atoms in Molecules, a Quantum Theory*; Clarendon Press: Oxford, U.K., 1990.

(4) (a) Streitwieser, A., Jr.; Williams, J. W.; Alexandratos, S.; McKelvey, J. M. *J. Am. Chem. Soc.* **1976**, *98*, 4778. (b) Ritchie, J. P.; Bachrach, S. M. *J. Am. Chem. Soc.* **1987**, *109*, 5909. (c) Hiberty, P. C.; Cooper, D. L. *J. Mol. Struct. (Theochem)* **1988**, *169*, 437. (d) Cioslowski, J. *J. Am. Chem. Soc.* **1989**, *111*, 8333.

(5) Kaufmann, E.; Raghavachari, K.; Reed, A. E.; Schleyer, P. v. R. *Organometallics* **1988**, *7*, 1597.

S0276-7333(95)00966-6 CCC: $12.00

Chart 1

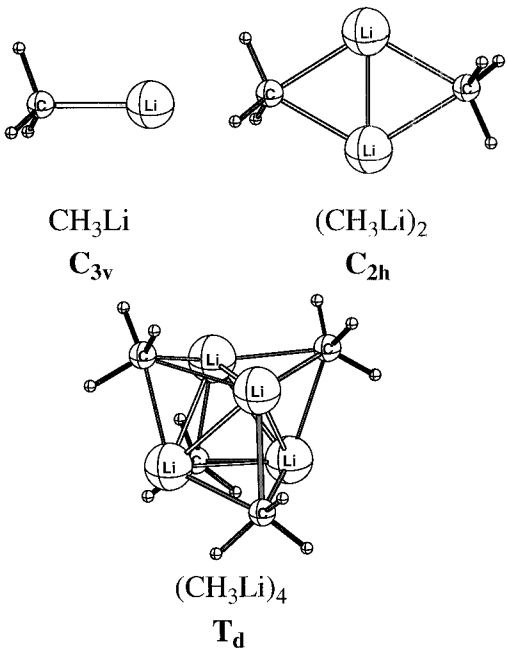

CH_3Li $(CH_3Li)_2$

C_{3v} C_{2h}

$(CH_3Li)_4$

T_d

carbanions, bound predominantly by electrostatic forces (**1**). Streitwieser[6a] and Bushby[6b,c] showed that even a simple electrostatic model already reproduces the ratio of C−C and Li−Li distances in tetrameric methyllithium.

Nevertheless, the details of the bonding within oligomers of lithium compounds are more complicated than follows from a simple electrostatic consideration:[7] Streitwieser's ideal distance ratio is not found for $(LiH)_4$, $(LiOH)_4$, and $(LiF)_4$, and for the latter two tetramers, a point charge model erroneously predicts that a planar eight-membered ring would be more stable than a tetrahedral structure.[7] The shared electron density between lithium and carbon, albeit small, is not negligible, which indicates that covalent contributions (**2**) to the bonding cannot be disregarded.[4a,8] Also, the sizable carbon−lithium NMR coupling constants of up to 17 Hz observed for organolithium aggregates[9] can be taken as evidence for the importance of covalent character (**2**) in the C−Li bond. Further, the bonding within the Li_n core of the aggregates is difficult to describe in the electrostatics-only picture.

In the present paper we investigate CH_3Li, $(CH_3Li)_2$, and $(CH_3Li)_4$ (Chart 1) using high levels of density-functional (DFT)[10] and conventional *ab initio*[11] theory. The calculations were carried out with the ADF[12,13] and Gaussian programs.[14] The purpose is to try to clarify some open points concerning the bonding in organolithium oligomers. In particular, we wish to obtain a better understanding of the nature of the carbon−lithium bond in these compounds. To what extent can it be conceived as a polar C−Li electron pair bond? Does it contain distinct covalent components? What is the role of the Li 2p orbitals (see ref 15), and what is the electronic structure of the Li_n cores? To answer these questions a detailed analysis of the bonding mechanism between the $(CH_3^{\bullet})_n$ and $(Li^{\bullet})_n$ fragments in $(CH_3-Li)_n$ has been carried out using the extended transition state (ETS) scheme developed by Ziegler and Rauk.[13] Furthermore, we analyze the bonding between the methyl radicals in the $(CH_3^{\bullet})_n$ "cages" and between the $Li^{\bullet}$ atoms in the $(Li^{\bullet})_n$ clusters (n = 2, 4). This enables us to interpret our quantitative results in physically meaningful terms from MO theory[16] and to provide insights, complementary to those obtained by common population analysis[2] and topological[3] methods.

2. Methods

A. Conventional *ab Initio* Computations. *Ab initio* calculations were performed using the Gaussian program package.[14] Structures were optimized at RHF/6-31+G* and RMP2(full)/6-31+G* (i.e. with all electrons included in the correlation treatment). Zero point vibrational energies (ZPE) were evaluated in frequency calculations at RHF/6-31+G*. These confirmed that all structures are minima. Atomic charges and delocalization energies were evaluated using the natural population analysis (NPA) and natural bond orbital

(6) (a) Streitwieser, A., Jr. *J. Organomet. Chem.* **1978**, *156*, 1. (b) Bushby, R. J.; Steel, H. L. *J. Organomet. Chem.* **1987**, *336*, C25. (c) Bushby, R. J.; Steel, H. L. *J. Chem. Soc., Perkin Trans. 2* **1990**, 1143.

(7) Sapse, A. M.; Raghavachari, K.; Schleyer, P. v. R.; Kaufmann, E. *J. Am. Chem. Soc.* **1985**, *107*, 6483. See also: Rupp, M.; Ahlrichs, R. *Theor. Chim. Acta.* **1977**, *46*, 117.

(8) (a) Graham, G. D.; Marynick, D. S.; Lipscomb, W. N. *J. Am. Chem. Soc.* **1980**, *102*, 4572. (b) Schiffer, H.; Ahlrichs, R. *Chem. Phys. Lett.* **1986**, *124*, 172.

(9) (a) Günther, H.; Moskau, D.; Bast, P.; Schmalz, D. *Angew. Chem.* **1987**, *99*, 1242; *Angew. Chem., Int. Ed. Engl.* **1987**, *26*, 1212. (b) Bauer, W.; Schleyer, P. v. R. *Adv. Carbanion Chem.* **1992**, *1*, 89. (c) Bauer, W. In *Lithium Chemistry*; Sapse, A. M., Schleyer, P. v. R., Eds.; Wiley-Interscience: New York, 1995; Chapter 5. (d) Fraenkel, G.; Martin, K. V. *J. Am. Chem. Soc.* **1995**, *117*, 10336.

(10) (a) Dreizler, R. M.; Gross, E. K. U. *Density Functional Theory, An Approach to the Quantum Many-Body Problem*; Springer-Verlag: Berlin, 1990. (b) Parr, R. G.; Yang, W. *Density-Functional Theory of Atoms and Molecules*; Oxford University Press: New York, 1989. (c) Slater, J. C. *Quantum Theory of Molecules and Solids*; McGraw-Hill: New York, 1974; Vol. 4.

(11) (a) Hehre, W. J.; Radom, L.; Schleyer, P. v. R.; Pople, J. A. *Ab Initio Molecular Orbital Theory*; Wiley-Interscience: New York, 1986. (b) McWeeny, R. *Methods of Molecular Quantum Mechanics*; Academic Press: London, 1992.

(12) (a) Fonseca Guerra, C.; Visser, O.; Snijders, J. G.; te Velde, G.; Baerends, E. J. Parallelisation of the Amsterdam Density Functional Program. In *Methods and Techniques for Computational Chemistry*; Clementi, E., Corongiu, G., Eds.; STEF: Cagliari, Italy, 1995; pp 305−395. (b) Baerends, E. J.; Ellis, D. E.; Ros, P. *Chem. Phys.* **1973**, *2*, 41. (c) Baerends, E. J.; Ros, P. *Int. J. Quantum Chem., Quantum Chem. Symp.* **1978**, *S12*, 169. (d) Ravenek, W. In *Algorithms and Applications on Vector and Parallel Computers*; Riele, H. H. J., Dekker, Th. J., van de Vorst, H. A., Eds.; Elsevier: Amsterdam, 1987. (e) Boerrigter, P. M.; te Velde, G.; Baerends, E. J. *Int. J. Quantum Chem.* **1988**, *33*, 87. (f) te Velde, G.; Baerends, E. J. *J. Comp. Phys.* **1992**, *99*, 84. (g) Snijders, J. G.; Baerends, E. J.; Vernooijs, P. *At. Nucl. Data Tabl.* **1982**, *26*, 483. (h) Krijn, J.; Baerends, E. J. *Fit-Functions in the HFS-Method, Internal Report* (in Dutch); Vrije Universiteit: Amsterdam, The Netherlands, 1984. (i) Vosko, S. H.; Wilk, L.; Nusair, M. *Can. J. Phys.* **1980**, *58*, 1200. (j) Becke, A. D. J. *Chem. Phys.* **1986**, *84*, 4524. (k) Becke, A. D. *Phys. Rev. A* **1988**, *38*, 3098. (l) Perdew, J. P. *Phys. Rev. B* **1986**, *33*, 8822. Erratum: *Ibid.* **1986**, *34*, 7406. (m) Fan, L.; Ziegler, T. *J. Chem. Phys.* **1991**, *94*, 6057.

(13) (a) Bickelhaupt, F. M.; Nibbering, N. M. M.; van Wezenbeek, E. M.; Baerends, E. J. *J. Phys. Chem.* **1992**, *96*, 4864. (b) Ziegler, T.; Rauk, A. *Inorg. Chem.* **1979**, *18*, 1558. (c) Ziegler, T.; Rauk, A. *Inorg. Chem.* **1979**, *18*, 1755. (d) Ziegler, T.; Rauk, A. *Theoret. Chim. Acta* **1977**, *46*, 1.

(14) Gaussian 94, Revision C.3: Frisch, M. J.; Trucks, G. W.; Schlegel, H. B.; Gill, P. M. W.; Johnson, B. G.; Robb, M. A.; Cheeseman, J. R.; Keith, T.; Petersson, G. A.; Montgomery, J. A.; Raghavachari, K.; Al-Laham, M. A.; Zakrzewski, V. G.; Ortiz, J. V.; Foresman, J. B.; Cioslowski, J.; Stefanov, B. B.; Nanayakkara, A.; Challacombe, M.; Peng, C. Y.; Ayala, P. Y.; Chen, W.; Wong, M. W.; Andres, J. L.; Replogle, E. S.; Gomperts, R.; Martin, R. L.; Fox, D. J.; Binkley, J. S.; Defrees, D. J.; Baker, J.; Stewart, J. P.; Head-Gordon, M.; Gonzalez, C.; Pople, J. A. Gaussian, Inc., Pittsburgh, PA, 1995.

(15) (a) Clark, T.; Rohde, C.; Schleyer, P. v. R. *Organometallics* **1983**, *2*, 1344. (b) Kost, D.; Klein, J.; Streitwieser, A.; Schriver, G. W. *Proc. Natl. Acad. Sci. U.S.A.* **1982**, *79*, 3922.

(16) (a) Albright, T. A.; Burdett, J. K.; Whangbo, M.-H. *Orbital Interactions in Chemistry*; Wiley-Interscience: New York, 1985. (b) Gimarc, B. M. *Molecular Structure and Bonding*; Academic Press: New York, 1979. (c) Rauk, A. *Orbital Interaction Theory of Organic Chemistry*; Wiley-Interscience: New York, 1994.

analysis (NBO) methods developed by Weinhold *et al.*[2] Aggregation energies were computed at the MP4SDQ/6-31+G* level; the calculation of the contributions of triple excitations (necessary for the complete MP4SDTQ energy) was not possible for the methyllithium tetramer due to technical (disk space) limitations.

B. Density-Functional Computations. The density-functional calculations were performed using the Amsterdam-Density-Functional (ADF) program developed by Baerends *et al.*[12,13] The MOs were expanded in an uncontracted set of Slater type orbitals (STOs) containing diffuse functions.[12g] The basis is of triple-ζ quality, augmented with two polarization functions: 2p and 3d on H; 3d and 4f on Li and C. In addition, the Li basis carries a 2p function. The basis set superposition error (BSSE) is expected to be negligible for this very large basis set (e.g. the BSSE for the CH_3-Li bond energy is only 0.2 kcal/mol). The 1s core shells of lithium and carbon were treated by the frozen-core approximation.[12b] An auxiliary set of s, p, d, f, and g STOs was used to fit the molecular density and to represent the Coulomb and exchange potentials accurately in each SCF cycle.[12h] The numerical integration was performed using the procedure developed by te Velde *et al.*[12e,f]

Energies were evaluated at the MP2(full)/6-31+G* equilibrium geometries using gradient corrected density functionals (NL-SCF).[12m] Exchange is described by Slaters Xα potential[10c] with nonlocal corrections due to Becke.[12j,k] Correlation is treated in the Vosko−Wilk−Nusair (VWN) parametrization[12i] with nonlocal corrections proposed by Perdew.[12l]

C. Analysis of Bonding Mechanisms. The C−Li bonding mechanism in the $(CH_3Li)_n$ species was analyzed using an extended transition state (ETS) method due to Ziegler and Rauk.[13] This was done at the NL-P level (nonlocal corrections added as a perturbation to the LDA result) for technical reasons. The NL-P analysis results are scaled to fit the bond energies with the corresponding NL-SCF values (which differ consistently by a few kcal/mol) to facilitate a straightforward comparison. The overall bond energy ΔE corresponds to the formation of $(CH_3Li)_n$ from the corresponding methyl and lithium radicals and is made up of two major components (eq 1).

$$n\mathrm{CH_3^\bullet} + n\mathrm{Li^\bullet} \rightarrow (\mathrm{CH_3{-}Li})_n \qquad \Delta E = \Delta E_{\mathrm{int}} + \Delta E_{\mathrm{prep}} \tag{1}$$

The preparation energy ΔE_{prep} is the amount of energy required to form the $(CH_3^\bullet)_n$ cage (eq 2) and the $(Li^\bullet)_n$ cluster

$$n\mathrm{CH_3^\bullet} \rightarrow (\mathrm{CH_3^\bullet})_n \qquad \Delta E_{\mathrm{prep}}((\mathrm{CH_3^\bullet})_n) \tag{2}$$

$$n\mathrm{Li^\bullet} \rightarrow (\mathrm{Li^\bullet})_n \qquad \Delta E_{\mathrm{prep}}((\mathrm{Li^\bullet})_n) \tag{3}$$

$$(\mathrm{CH_3^\bullet})_n + (\mathrm{Li^\bullet})_n \rightarrow (\mathrm{CH_3{-}Li})_n \qquad \Delta E_{\mathrm{int}} \tag{4}$$

(eq 3) in the geometry which they acquire in the overall molecule. The interaction energy ΔE_{int} corresponds to the actual energy change when the prepared $(CH_3^\bullet)_n$ and $(Li^\bullet)_n$ fragments are combined to form the C−Li bond (eq 4).

The interaction energy is further split up into three physically meaningful terms (eq 5).[13] The term ΔE_{elst} corresponds

$$\Delta E_{\mathrm{int}} = \Delta E_{\mathrm{elst}} + \Delta E_{\mathrm{Pauli}} + \Delta E_{\mathrm{oi}} = \Delta E^0 + \Delta E_{\mathrm{oi}} \tag{5}$$

to the classical electrostatic interaction between the unperturbed charge distributions of the prepared fragments and is usually attractive. The Pauli-repulsion $\Delta E_{\mathrm{Pauli}}$ comprises the 3- and 4-electron destabilizing interactions between occupied orbitals and is responsible for the steric repulsion. For neutral fragments, it is useful to combine ΔE_{elst} and $\Delta E_{\mathrm{Pauli}}$ in the steric interaction ΔE^0 (eq 5).

The orbital interaction ΔE_{oi} accounts for formation of electron pair bonds, charge transfer (interaction between occupied orbitals on one moiety with unoccupied orbitals of the other) and polarization (empty/occupied orbital mixing on one fragment). It can be split up into the contributions from each irreducible representation Γ of a $(CH_3Li)_n$ system (eq 6).

$$\Delta E_{\mathrm{oi}} = \sum_{\Gamma} \Delta E_{\Gamma} = \Delta E_{\mathrm{low}} + \Delta E_{\mathrm{high}} + \Delta E_{\mathrm{rest}} \tag{6}$$

In the present work, two dominant contributions can be recognized. Therefore, we have partitioned the orbital interactions as follows (eq 6): (i) ΔE_{low}, the contribution from the symmetry in which a lower energy SOMO ($SOMO_{\mathrm{low}}$; see Figures 2, 3, and 6) on $(CH_3^\bullet)_n$ and another one on $(Li^\bullet)_n$ interact; (ii) ΔE_{high}, the contribution from the symmetry in which a higher energy SOMO ($SOMO_{\mathrm{high}}$) on $(CH_3^\bullet)_n$ and another one on $(Li^\bullet)_n$ interact; (iii) ΔE_{rest}, a rest term containing the contributions from the remaining symmetries. For CH_3Li, there is only one SOMO on each fragment ($CH_3^\bullet$ and $Li^\bullet$) which is assigned as $SOMO_{\mathrm{low}}$.

The C−Li bond in CH_3Li has also been analyzed heterolytically (i.e. in terms of the interaction between the CH_3^- and Li^+ fragments). This facilitates the comparison with the NBO analysis in which in a first step the bonding electron pair is localized for 100% as a lone pair on methyl (Lewis structure) followed by a second step which allows for delocalization.

D. Charge Distribution. DFT atomic charges were obtained using four different procedures: (1) the Hirshfeld scheme;[17a] (2) an electron density partitioning scheme, discussed below, which we term Voronoi deformation density; (3) the Mulliken scheme;[17b] (4) a modification to the Mulliken scheme, discussed below, which we designate modified Mulliken (NPA and other methods for the calculation of atomic charges are not available within the ADF program). In the Hirshfeld method, a hypothetical promolecule with electron density $\sum\rho_{\mathrm{B}}$ is constructed by the superposition of spherically symmetrized charge densities ρ_{B} of the isolated atoms B. The electron density ρ of the real molecule at each point in space is then distributed over the atoms A in the same ratio $w_{\mathrm{A}} = (\rho_{\mathrm{A}}/\sum\rho_{\mathrm{B}})$ as they contribute charge density to that point in the promolecule. The Hirshfeld atomic charge $Q_{\mathrm{A}}^{\mathrm{H}}$ is obtained by subtracting the resulting partial density associated with atom A from the corresponding nuclear charge Z_{A} (eq 7). The Hirshfeld scheme accounts in a natural way for the fact that each type of atom has a certain, characteristic effective size.

$$Q_{\mathrm{A}}^{\mathrm{H}} = Z_{\mathrm{A}} - \int w_{\mathrm{A}}(r)\,\rho(r)\,\mathrm{d}r^3 \tag{7}$$

The Voronoi deformation density (VDD) approach is based on the partitioning of space into the Voronoi cells of each atom A, i.e. the region of space that is closer to that atom than to any other atom (cf. Wigner−Seitz cells in crystals).[12f] The VDD charge of an atom A is then calculated as the difference between the (numerical) integral of the electron density ρ of the real molecule and the superposition of atomic densities $\sum\rho_{\mathrm{B}}$ of the promolecule (*vide supra*) in its Voronoi cell (eq 8).

$$Q_{\mathrm{A}}^{\mathrm{VDD}} = -\int_{\substack{\mathrm{Voronoi}\\ \mathrm{cell\ A}}} [\rho(r) - \sum_{\mathrm{B}} \rho_{\mathrm{B}}(r)]\,\mathrm{d}r^3 \tag{8}$$

Thus, the VDD atomic charges are a way to quantify the deformation density $\rho - \sum\rho_{\mathrm{B}}$ on an atomic basis using a simple geometric partitioning of space. They merely monitor if charge "flows" away or toward the space around a certain nucleus upon the formation of the molecule from its atoms. Therefore, the physical interpretation is rather simple and straightforward: a positive or negative atomic charge Q_{A} corresponds to the loss or gain of electrons in the Voronoi cell of atom A.

The Mulliken method makes use of the basis functions which are used to represent the wavefunction. Gross Mulliken

(17) (a) Hirshfeld, F. L. *Theor. Chim. Acta* **1977**, *44*, 129. (b) Mulliken, R. S. *J. Chem. Phys.* **1955**, *23*, 1833.

Table 1. Geometries, Energies, and NPA/NBO Analysis Data for Methyllithium Oligomers[a]

	CH_3Li	$(CH_3Li)_2$	$(CH_3Li)_4$
MP2(full) Geometries (Å, deg)			
C−Li	2.005	2.105, 2.128	2.188
Li−Li		2.147	2.363
C−C		3.649	3.582
C−H	1.099	1.104	1.107
∠H−C−H	107.3	103.7, 105.8	102.9
Energies (au or kcal/mol)			
E_{MP4SDQ}	−47.183 74	−94.437 42	−188.953 23
ZPE[b]	22.1	45.4	94.4
$\Delta E_{oligo}+\Delta ZPE$[b]		−42.8	−131.5
E_{MP4SDQ} (Li(s only))	−47.170 80	−94.400 38	−188.858 68
$\Delta E_{oligo}+\Delta ZPE$[b] (Li(s only))		−35.8	−104.6
NPA Lithium Charge (e)			
HF	+0.86	+0.89	+0.87
MP4SDQ	+0.85	+0.88	+0.86
Delocalization Energies from Fock−Matrix Deletion (kcal/mol)[c]			
$(CH_3)_n \rightarrow (Li)_n$	31	92	273
Delocalization Energies from 2nd-Order Estimate (kcal/mol)[c]			
$LP_C \rightarrow Li(s)$[d]	54	96	282
$LP_C \rightarrow Li(p)$[d]	7	12	22
$Bd_{CH} \rightarrow Li(s)$[d]	2	9	64
tot. 2nd-order est	63	117	368

[a] The 6-31+G* basis was used unless stated otherwise. [b] ZPEs from HF/6-31+G* frequencies. [c] Calculated at HF/6-31+G*. [d] Estimated using second-order perturbation theory.

Atomic charges Q_A are obtained as follows: (1) the overlap populations in terms of the primitive basis functions q_{ij} are divided half-and-half between the corresponding orbital populations q_{ii} and q_{jj} (eq 9); (2) the resulting diagonal elements q_{ii}' which belong to the same atom A are summed and subtracted from the corresponding nuclear charge Z_A (eq 10).

$$q_{ii}' = q_{ii} + \sum_{j(\neq i)} {}^1/_2(q_{ij} + q_{ji}) \tag{9}$$

$$Q_A{}^M = Z_A - \sum_{i \in A} q_{ii}' \tag{10}$$

The choice to divide overlap populations half-and-half is arbitrary and tends to cause an unrealistic buildup of charge density on electropositive atoms. In the closely related modified Mulliken method, we try to reduce these well-known problems by dividing the overlap populations q_{ij} between the corresponding orbital populations q_{ii} and q_{jj} in the ratio between the latter (eq 11). This choice, although still arbitrary, relates the partitioning in some way to the electronegativity difference between the corresponding atoms.

$$q_{ii}' = q_{ii} + \sum_{j(\neq i)} \left(\frac{q_{ii}}{q_{ii} + q_{jj}} \right) (q_{ij} + q_{ji}) \tag{11}$$

3. Results and Discussion

In the following the results of the conventional *ab initio* computations and the NBO analysis are discussed (section 3A). Thereafter, we discuss the DFT results for methyllithium oligomerization and carbon−lithium bond energies together with the results of the electronic structure and C−Li bonding analysis (section 3B).

A. *Ab Initio* Results and NBO Analysis. Oligomerization of Methyllithium. The structures of the methyllithium monomer, dimer, and tetramer are shown in Chart 1. Geometry parameters (MP2(full)/6-31+G*), energies (MP4SDQ), and selected results from the NBO analysis are given in Table 1. The main features of the geometries of the methyllithium oligomers have been discussed previously, on the basis of Hartree−Fock structures.[5,18] Geometry optimization at correlated levels causes the C−Li and Li−Li distances to become somewhat shorter, but very little change is observed otherwise. The pyramidalization of the methyl groups increases upon going to the larger oligomers.

The ΔZPE-corrected MP4SDQ/6-31+G* dimerization energy of −42.8 kcal/mol ($\Delta E_{oligo}+\Delta ZPE$, Table 1) obtained in the present study is slightly lower than the published "best estimate" of −44.3 kcal/mol.[5] On the other hand, the energy calculated for tetramerization, 131.5 kcal/mol, is larger than the extrapolated value of 122.9 kcal/mol.[5] Oligomerization of organolithium compounds is thus highly exothermic and leads to tightly bound aggregates which often resist breaking apart even in ethereal solution. Recently, Ogle *et al.*[19a] determined a heat of combustion of crystalline $[CH_3Li\cdot THF]_4$ of 9400 ± 300 cal/g and, based on the basis of this result, calculated, a ΔH_f of −196 kcal/mol for this compound with an error interval of ±113 kcal/mol. Using our calculated gas-phase ΔH_f for CH_3Li of +29.2 kcal/mol (*vide infra*), the aforementioned tetramerization energy of −131.5 kcal/mol, the experimental ΔH_f for THF, −51.67 kcal/mol,[19b] and assuming a Li−THF interaction energy of −15.9 kcal/mol (the calculated interaction energy between $(CH_3Li)_4$ and $(CH_3)_2O$[19c]), we estimate a ΔH_f of −285 kcal/mol for gas-phase $[CH_3Li\cdot THF]_4$.

Nowadays, organolithium oligomers are generally considered as aggregates of lithium cations and carbanions, bound mainly by electrostatic forces. Indeed, an electrostatic description as proposed by Streitwieser,[6a] and by Bushby and Steel,[6b,c] is well capable of rationalizing the structural features. The results of the natural population analysis (NPA) are in line with this view of a predominantly ionic character of the C−Li bond (Table 1). The NPA lithium charges are high, +0.85 to +0.88 e, and independent of the size of the aggregate (the value for the dimer is only slightly higher than for the monomer and the tetramer). Inclusion of correlation also has very little influence on the NPA charge distribution.

Importance of Lithium 2p Orbitals. The difference in orbital energy between lithium 2s and 2p orbitals is relatively small (see Figure 2). This indicates that the 2p AOs of lithium can be regarded as valence orbitals. The often significant contributions of p-functions to the bonding in organolithium oligomers in calculations employing (according to modern standards) relatively small basis sets had been taken as evidence for largely covalent carbon−lithium bonding.[20] On the other hand, Clark *et al.*[15a] and Streitwieser *et al.*[15b] have argued that p-type functions on lithium act in many cases as "superposition functions"; i.e., they serve only to improve the description of the organic fragments, instead of contributing to the description of the carbon−lithium bond itself. They showed that calculations

(18) van Eikema Hommes, N. J. R.; Schleyer, P. v. R. *J. Am. Chem. Soc.* **1992**, *114*, 1146.
(19) (a) Ogle, C. A.; Huckabee, B. K.; Johnson, H. C., IV; Sims, P. F.; Winslow, S. D.; Pinkerton, A. A. *Organometallics* **1993**, *12*, 1960 and references cited therein. (b) *Lange's Handbook of Chemistry*, 13th ed.; Dean, J. A., Ed.; McGraw-Hill Book Co.: New York, 1985. (c) van Eikema Hommes, N. J. R.; Schleyer, P. v. R. Manuscript in preparation.
(20) (a) Guest, M. F.; Hillier, I. H.; Saunders, V. R. *J. Organomet. Chem.* **1972**, *44*, 59. (b) Baird, N. C.; Barr, R. F.; Datta, R. K. *J. Organomet. Chem.* **1973**, *59*, 65. (c) Hincliffe, A.; Saunders, E. J. *J. Mol. Struct.* **1976**, *31*, 283.

using a truncated basis set on lithium, with only s-type basis functions, yielded essentially the same results (including the energetic ordering of isomers) as calculations using the full basis sets and concluded that bonding in organolithium species is governed by electrostatic interactions.

In the present work, we have used the extended 6-31+G* basis set in the evaluation of the aggregation energies. This basis set is expected to be of sufficient quality to largely eliminate the effects of basis set superposition error (BSSE).[21] Therefore, the omission of p-type functions from the Li basis should have no significant influence on the aggregation energies if lithium 2p orbitals were unimportant for the description of the intra-aggregate bonding. Our results (Table 1) show that this is not the case. The oligomerization energies ΔE_{oligo}+ΔZPE calculated with the truncated basis set are up to 20% lower than those obtained using the full 6-31+G* basis. Obviously, the bonding mechanism in the methyllithium aggregates is more complicated than suggested by an electrostatics-only picture (see also section 3B).

NBO Analysis. One of the features of the NBO analysis program is the possibility to consider the wave function of a molecule in terms of delocalizations from an "ideal" Lewis structure. For the Hartree−Fock wave function, the energy associated with such delocalizations can be evaluated by explicit deletion of the delocalizations (by means of zeroing the corresponding off-diagonal elements in the Fock matrix expressed in NBOs) and recomputation of the energy or through a second-order perturbational method. The results from the perturbational treatment generally overestimate the delocalization energies.[2b] It is not possible to perform a similar energetic analysis based on a correlated wave function.

Three contributions are important in the intra-aggregate bonding: (1) delocalization from the carbon lone pair NBO into lithium 2s orbitals; (2) delocalization from the carbon lone pair NBO into lithium 2p orbitals; (3) "agostic" delocalizations from C−H bond NBOs into lithium 2s orbitals. Other delocalizations have only minor contributions. A detailed analysis of the contributions from agostic interactions has been given previously.[5]

The calculated deletion energies for removal of all delocalizations between the methyl and lithium moieties, together with the second-order energy estimates for the aforementioned delocalizations, are given in Table 1. The larger contribution from agostic delocalizations in the tetramer of 64 kcal/mol, compared to the published value of 44 kcal/mol,[5] is due to the shorter Li−H distances in the MP2(full)6-31+G* optimized structures used in the present study.

Removal of all delocalizations between the methyl and lithium fragments leads to an essentially ionic bonding model. The corresponding delocalization energy can be interpreted as the stabilization due to covalent bonding between carbon and lithium. As expected (*vide supra*), this energy is overestimated in the perturbational treatment, but also the delocalization energy calculated by Fock matrix deletion, 31 kcal/mol, is probably somewhat too high, since the methyl fragments are not allowed to relax in response to the change in electron distribution due to the deletion. This neglect of relaxation may also contribute to the difference between the deletion energy, 31 kcal/mol, and the orbital interaction energy ΔE_{oi}, 21 kcal/mol, obtained in the "ionic" ETS analysis of methyllithium monomer, discusssed in the following section.

(21) (a) See, e.g.: Hobza, P.; Zahradnik, R. *Chem. Rev.* **1988**, *88*, 871. (b) The stabilization of the $(CH_3)_n$ fragment upon the introduction of lithium ghost orbitals for n = 1, 2, and 4 using the geometries of the corresponding $(CH_3Li)_n$ systems (counterpoise method) is very small, namely −0.4, −1.1, and −2.8 kcal/mol, and the corresponding charge transfer to lithium of 0.002, 0.003, and 0.006 e is in fact negligible.

Table 2. Analysis of the C−Li Bonding Mechanism in $(CH_3Li)_n$[a]

	$CH_3^- + Li^+$	$CH_3^\bullet + Li^\bullet$	$(CH_3Li)_2$[b]	$(CH_3Li)_4$[c]
		Energy (kcal/mol)[d]		
ΔE_{low}	−15.0	−62.9	−92.8	−85.8
ΔE_{high}			−138.0	−387.0
ΔE_{rest}	−5.9	−1.0	−3.2	−18.7
ΔE_{oi}	−20.9	−63.9	−234.0	−491.5
ΔE_{Pauli}	45.0	40.1	258.0	520.8
ΔE_{elst}	−198.9	−32.1	−200.0	−401.3
ΔE_{int}	−174.8	−55.9[e]	−176.0	−372.0
$\Delta E_{prep}((CH_3)_n)$	0.6	10.4	29.2	66.7
$\Delta E_{prep}((Li)_n)$	0.0	0.0	14.1	−3.3
ΔE	−174.2	−45.5	−132.7	−308.6
ΔE_{oligo}[f]			−41.7	−126.6
		Fragment Orbital Overlaps[g]		
$(CH_3)_n + (Li)_n$				
$\langle SOMO_{low}\|SOMO_{low}\rangle$		0.33	0.47	0.55
$\langle SOMO_{high}\|SOMO_{high}\rangle$			0.26	0.29
$CH_3 + CH_3'$: $\langle 2a_1\|2a_1\rangle$			0.10	0.09
Li + Li′				
$\langle 2s\|2s\rangle$			0.69	0.65
$\langle 2p_z\|2p_z\rangle$			0.01	0.23
$\langle 2p_\pi\|2p_\pi\rangle$			0.58	
		Fragment Orbital Populations (e)[h]		
$(CH_3)_n$				
$P(SOMO_{low})$		1.40	1.36	1.02
$P(SOMO_{high})$			1.52	1.43[i]
$(Li)_n$				
$P(SOMO_{low})$		0.50	0.57	0.91
$P(SOMO_{high})$			0.63	0.65[i]

[a] NL-SCF/TZ2P//MP2(full)/6-31+G*. ΔE_{int} decomposition: NL-P/TZ2P scaled to fit with NL-SCF/TZ2P result. [b] $(CH_3^\bullet)_2 + (Li^\bullet)_2$. [c] $(CH_3^\bullet)_4 + (Li^\bullet)_4$. [d] $\Delta E = \Delta E_{int} + \Delta E_{prep} = \Delta E_{oi} + \Delta E_{Pauli} + \Delta E_{elst} + \Delta E_{prep}$ (section 2.B); ΔE = overall energy change for formation of $(CH_3Li)_n$ from CH_3 and Li ions or radicals; ΔE_{int} = interaction between $(CH_3)_n$ and $(Li)_n$ fragments; ΔE_{prep} = preparation energy required to form the $(CH_3)_n$ and $(Li)_n$ fragments from the corresponding CH_3 and Li ions or radicals; ΔE_{elst} = classical electrostatic interaction between the unperturbed charge distributions of the $(CH_3)_n$ and $(Li)_n$ fragments; ΔE_{Pauli} = Pauli repulsion between occupied fragment orbitals; $\Delta E_{oi} = \Delta E_{low} + \Delta E_{high} + \Delta E_{rest}$ = orbital interaction, composed of the electron pair bond of the lower and higher energy SOMOs of the $(CH_3)_n$ and $(Li)_n$ fragments plus a rest term. [e] BSSE of 0.2 kcal/mol was neglected. [f] ΔE_{oligo} = oligomerization energy of CH_3Li. [g] Overlaps between orbitals of the indicated fragments. [h] $P(\varphi)$ is the gross Mulliken population which fragment orbital φ carries in the overall molecule. [i] Population of one member to the triple degenerate T_2 set.

B. DFT Results and Analysis of Bonding Mechanisms. Oligomerization of CH_3Li and C−Li Bond Energies. The results of the density-functional calculations are summarized in Tables 2 and 3 (energies and bonding analysis) and Figures 1−6 (electronic structure). The energy gain ΔE associated with the formation of $(CH_3{-}Li)_n$ from n $Li^\bullet$ and n $CH_3^\bullet$ radicals is −45.5, −132.7, and −308.6 kcal/mol for n = 1, 2, and 4, computed using nonlocal density-functionals and a large, doubly polarized triple-ζ STO basis (NL-SCF/TZ2P). This gives a bond dissociation energy $D_0(CH_3{-}Li)$ = 43.5 kcal/mol for methyllithium (ΔZPE = −2.0,

Table 3. Carbon and Lithium Charges (e) in Methyllithium Oligomers[a]

	CH_3Li		$(CH_3Li)_2$		$(CH_3Li)_4$	
	C	Li	C	Li	C	Li
Hirshfeld Method						
NL-SCF/DZ	−0.45	+0.51	−0.42	+0.43	−0.36	+0.32
NL-SCF/TZ2P	−0.43	+0.49	−0.40	+0.42	−0.34	+0.30
Voronoi Deformation Density Method						
NL-SCF/DZ	−0.33	+0.39	−0.36	+0.27	−0.34	+0.15
NL-SCF/TZ2P	−0.25	+0.38	−0.28	+0.26	−0.26	+0.13
Mulliken Method						
NL-SCF/DZ	−1.29	+0.56	−1.40	+0.61	−1.37	+0.54
NL-SCF/TZ2P	+0.12	+0.20	+0.20	+0.22	+0.42	+0.10
Modified Mulliken Method						
NL-SCF/DZ	−0.77	+0.80	−0.93	+0.86	−0.93	+0.80
NL-SCF/TZ2P	−0.05	+0.41	−0.24	+0.27	−0.30	+0.12

[a] Using MP2(full)/6-31+G* geometries.

NL-SCF/TZ2P), in good agreement with previous theoretical D_0 values of 42.1[5] and 43.7 kcal/mol.[8b] The corresponding 298.15 K bond dissociation enthalpy $\Delta H_{diss,298}(CH_3{-}Li)$ = 43.7 kcal/mol ($\Delta E_{therm} + \Delta pV$ = −1.8), which leads to a heat of formation $\Delta H_f(CH_3Li(g))$ = 29.2 kcal/mol, using the experimental heats of formation[22] of 34.8 ± 0.3 and 38.1 kcal/mol for $CH_3^\bullet$ and $Li^\bullet$, respectively. The BSSE is very small, only 0.2 kcal/mol, and is therefore neglected.

Table 2 gives the NL/TZ2P dimerization and tetramerization energies for methyllithium. Correction for zero point vibrational energy (computed at HF/6-31+G*) yields a dimerization energy of −40.6 kcal/mol and a tetramerization energy of −123.2 kcal/mol. The NL/TZ2P dimerization energy is in good agreement with the MP4SDQ/6-31+G* value of −42.8 kcal/mol (Table 1). Recently, Pratt and Kahn[23] calculated a dimerization energy of −48.9 kcal/mol using the local density approximation (LDA) and a double numeric basis with polarization functions (DZP); the stronger bonding, compared to our NL/TZ2P value of −40.6 kcal/mol, reflects the general tendency of LDA to lead to overbinding. The NL/TZ2P tetramerization energy is somewhat lower than the MP4SDQ/6-31+G* value of −131.5 kcal/mol (Table 1). The perfect agreement with the extrapolated value of −122.9 kcal/mol[5] is probably fortuitous.

Charge Distribution. Table 3 shows the carbon and lithium charges for the three methyllithium oligomers obtained using the Hirshfeld (H),[17a] Voronoi deformation density (VDD), Mulliken (M),[17b] and modified Mulliken (MM) methods (Section 2D). The calculations were performed at the NL-SCF level with the large TZ2P as well as a smaller, unpolarized double-ζ (DZ) STO basis to assess basis set dependencies.

First, we compare the general features of these approaches. The VDD and particularly the Hirshfeld method yield atomic charges which are essentially stable against basis set variations and correctly reflect the electronegativity differences between the atoms: negative carbon, essentially uncharged hydrogen and positive lithium. Both Mulliken population analyses display a strong basis set dependence. The Mulliken method yields rather unphysical atomic charges at NL-SCF/TZ2P: carbon carries a positive charge, in $(CH_3Li)_4$ even more positive than lithium! The situation improves in the modified Mulliken approach, where carbon remains negative in all cases. Similarly, modified Mulliken (MM) charges are more satisfactory than Mulliken (M) charges for the test series HF, LiF, H_2O, OH^-, and C_6H_6. However, both methods fail to yield chemically meaningful atomic charges for CH_4: $Q(C)_{NL\text{-}SCF/TZ2P}$ = +0.59 (M) and +0.02 e (MM) (for comparison, Hirshfeld yields −0.17 e). The modified Mulliken scheme might be an interesting alternative in extended Hückel computations in which basis set dependencies play no role (because of the use of a minimal basis set) and where Mulliken is still the standard method for calculating atomic charges. Summarizing, Hirshfeld is the most satisfactory method amongst these approaches with regard to the computation of chemically meaningful and basis set independent atomic charges.

The VDD lithium charges decrease from 0.38 via 0.26 to 0.13 e along CH_3Li, $(CH_3Li)_2$, and $(CH_3Li)_4$. This clearly shows that the shift of electron density from lithium to methyl decreases upon oligomerization. In agreement with this, the Hirshfeld lithium charges decrease from +0.49 via +0.42 down to +0.30 e (NL-SCF/TZ2P) along the same series of methyllithium oligomers. This trend also shows up in the increasing population of the $(Li^\bullet)_n$ fragment orbitals $SOMO_{low}$ and $SOMO_{high}$ (Table 2) and is indicative for the increasing importance of a covalent component in the carbon−lithium bond (*vide infra*). The pyramidalization of the methyl groups increases slightly upon oligomerization in spite of the decreasing negative charge (Tables 2 and 3); this may be ascribed to the increasing depopulation of the H−H antibonding methyl $1e_1$ orbitals (Figure 1), caused by "agostic" interactions with $(Li^\bullet)_n$. Note that the reduction of Li → CH_3 charge transfer upon oligomerization is not monitored by the NPA charges (Table 1). Note also that the carbon−lithium bond is much less ionic according to Hirshfeld ("50−30%") than according to NPA charges (ca. "90%").

We consider both the Hirshfeld and the NPA approach as satisfactory for the definition of basis set independent and chemically meaningful atomic charges (*cf.* Wiberg and Rablen and Meister and Schwarz).[24] The fact that there is nevertheless a significant discrepancy between the two methods demonstrates, in our opinion, that the degree of ionicity of a bond obtained on the basis of atomic charges should not be regarded as an absolute quantity. Instead, it is more meaningful to consider trends in atomic charges across a series of molecules using the same method, as has also been pointed out by Ahlrichs.[8b] The Voronoi deformation density (VDD) scheme may also be useful for the study of such trends because, in a sense unprejudiced, it merely monitors shifts in electron density from one region of space to another.

Methyllithium Monomer. The C−Li bonding mechanism in monomeric methyllithium can be analyzed in two ways: (1) homolytically, as an interaction between $CH_3^\bullet$ and $Li^\bullet$; (2) heterolytically, as an interaction between CH_3^- and Li^+. It is instructive to compare the two approaches.

First, the homolytic view is considered. The valence electronic structures of $CH_3^\bullet$ and $Li^\bullet$ are schematically shown in Figure 1. Lithium has a singly occupied 2s

(22) Lias, S. G.; Bartmess, J. E.; Liebman, J. F.; Holmes, J. L.; Levin, R. D.; Mallard, W. G. *J. Phys. Chem. Ref. Data* **1988**, *17*, Suppl. No. 1.
(23) Pratt, L. M.; Khan, I. M. *J. Comput. Chem.* **1995**, *16*, 1067.
(24) (a) Wiberg, K. B.; Rablen, P. R. *J. Comput. Chem.* **1993**, *14*, 1504. (b) Meister, J.; Schwarz, W. H. E. *J. Phys. Chem.* **1994**, *98*, 8245.

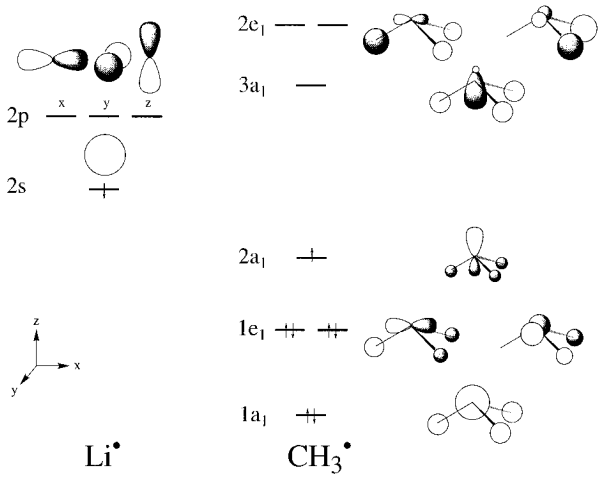

Figure 1. Valence MO scheme for Li• and CH_3•.

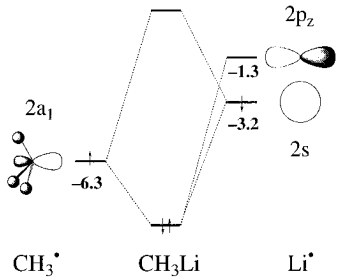

Figure 2. Orbital interaction diagram for CH_3Li.

orbital and a set of empty 2p AOs, only 2 eV higher in energy. The orbital spectrum of CH_3• consists of the doubly occupied $1a_1$ (σ_{C-H} bonding, involving carbon 2s) and $1e_1$ orbitals (σ_{C-H} bonding, involving carbon $2p_x$ and $2p_y$) and their antibonding counterparts, the $3a_1$ LUMO and $2e_1$ LUMO+1. The $2a_1$ SOMO (essentially nonbonding) is located in between.

In CH_3Li, the methyl $2a_1$ and the 3 eV higher energy lithium 2s enter in an strongly polar electron pair bond (Figure 2) as reflected by the increased population of the methyl $2a_1$: $P(SOMO_{low}) = 1.40$ e (Table 2). The significant overlap of 0.33 leads to a substantial $2a_1 \pm 2s$ mixing and is responsible for the covalent character of the C−Li bond, together with a sizable contribution of lithium $2p_z$ which acquires a population of 0.19 e (not shown in Table 2). The same $2p_z$ function is unoccupied in the calculation of the methyl radical in the presence of a ghost lithium atom using the geometry of CH_3Li. This shows that the lithium $2p_z$ orbital acts like a "normal" valence orbital in the description of the C−Li bond and not as a superposition function. The strong charge donation from Li to C is in line with the difference in electronegativity between these atoms and with the modern picture of a strongly polar carbon−lithium bond.[1] The gross Mulliken populations of the CH_3• and Li• orbitals and the Hirshfeld atomic or fragment charges display similar trends (Tables 2 and 3).

The orbital interaction ΔE_{oi} of −63.9 kcal/mol is almost exclusively provided by the polar electron pair bond ΔE_{low} (Table 2); a small contribution of −1.0 kcal/mol stems from a π-type interaction between C−H bonding $1e_1$ orbitals and lithium 2p. The orbital interactions are opposed by a steric repulsion $\Delta E_{Pauli} + \Delta E_{elst} = 8$ kcal/mol (mainly due to mutual core-valence overlap) and a preparation energy $\Delta E_{prep} = 10.4$ kcal/mol (caused by the pyramidalization of CH_3•), leading to the overall C−Li bond energy $\Delta E = -45.5$ kcal/mol.

Two striking changes occur on going to the heterolytic approach (Table 2): (1) the electrostatic interaction ΔE_{elst} increases from −32.1 to −198.9 kcal/mol; (2) the interaction ΔE_{low} between the methyl $2a_1$ (lone-pair on CH_3^-) and the lithium 2s (LUMO of Li^+) decreases from −62.9 to −15.0 kcal/mol. The increase of the electrostatic attraction is not unexpected as one goes from neutral to oppositely charged fragments: e.g., two point charges of +1 and −1 e separated by 2.005 Å yield an electrostatic attraction of −166 kcal/mol (our value of ca. −200 kcal/mol is even larger since the CH_3^- lone pair is oriented toward Li^+). The sizeable $2a_1 + 2s$ interaction of −15 kcal/mol (associated with a charge transfer of half an electron) is a quantitative measure for the tendency of methyllithium to deviate from the purely ionic structure **2**! In a sense, the orbital interactions ΔE_{oi} (−21 kcal/mol) in the heterolytic approach correspond to the orbital delocalizations (−31 kcal/mol) from the ionic Lewis structure **2** in the NBO analysis (*vide supra*). Note however that a straightforward comparison is not possible because of the fundamental differences between the interaction of canonic orbitals in MO theory[16] and orbital delocalizations of NBOs.[2]

Overall, the heterolytic dissociation of CH_3Li ($-\Delta E = 174.2$ kcal/mol) is ca. 4 times more endothermic than the homolytic dissociation ($-\Delta E = 45.5$ kcal/mol) due to the charge separation ($\Delta E_{prep}(CH_3)$ is essentially zero, a consequence of the pyramidal geometry of the methyl anion which is only subjected to minimal geometry changes in CH_3Li). In this respect, it seems more natural to conceive the carbon−lithium bond as a polar electron pair bond. This is also in line with the NL-SCF/TZ2P dipole moment of 5.6 D; a complete electron transfer from Li to C would lead to a dipole moment of 9.5 D, as pointed out before by Ahlrichs,[8b] who calculated a dipole moment of 5.7 D using the coupled pair functional (CPF) method. On the other hand, the heterolytic approach leads to a three times smaller orbital interaction ΔE_{oi} (Table 1) which can be associated with less charge reorganization and thus a better zeroth order picture at the equilibrium geometry. However, the heterolytic approach provides an unbalanced starting point for $(CH_3Li)_2$ and $(CH_3Li)_4$: excessive and unphysical electrostatic repulsions, especially between lithium cations (e.g. +843 kcal/mol for Li_4^{4+}), have to be compensated by even larger donor/acceptor and electrostatic interactions between the methyl anion cage and the lithium cation cluster. Therefore, we discuss the C−Li bond in the methyllithium dimer and tetramer solely in terms of the homolytic approach.

Methyllithium Dimer. Next, we consider the carbon−lithium bond in $(CH_3Li)_2$. The corresponding $(CH_3$•$)_2$ and $(Li$•$)_2$ fragments have triplet electronic structures with one electron in a C−C (or Li−Li) bonding ($SOMO_{low}$) and one electron in a C−C antibonding or Li−Li π bonding orbital ($SOMO_{high}$, Figure 3). The formation of the $(CH_3$•$)_2$ fragment from two CH_3• radicals is accompanied by a preparation energy of 29.2 kcal/mol, mainly due to methyl pyramidalization. The methyl−methyl repulsion is weak and the energy gap between $SOMO_{low}$ ($3a_g$, C−C bonding) and $SOMO_{high}$ ($3b_u$, C−C antibonding) is only 0.8 eV (Figure 3) due to the relatively long C−C distance of 3.65 Å (Table 1). The formation of triplet $(Li$•$)_2$ is also endothermic with

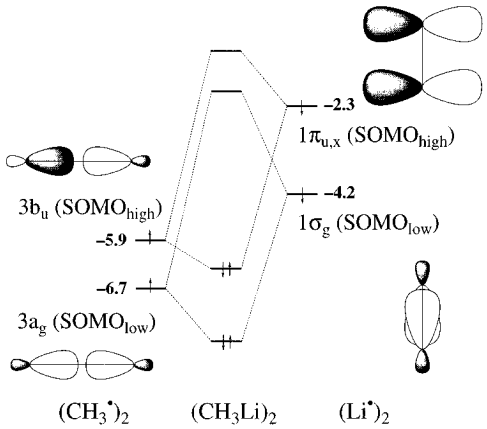

Figure 3. Orbital interaction diagram for $(CH_3Li)_2$.

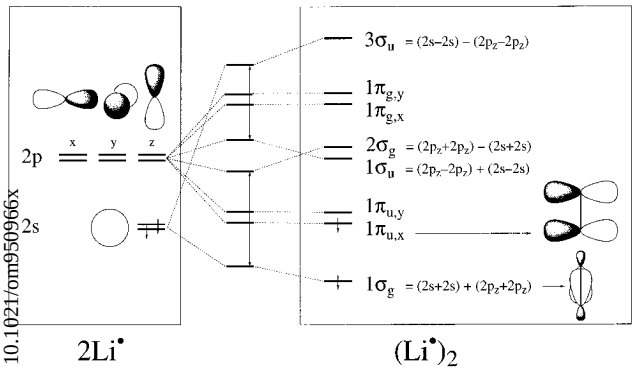

Figure 4. Orbital interaction diagram for $(Li^{\bullet})_2$.

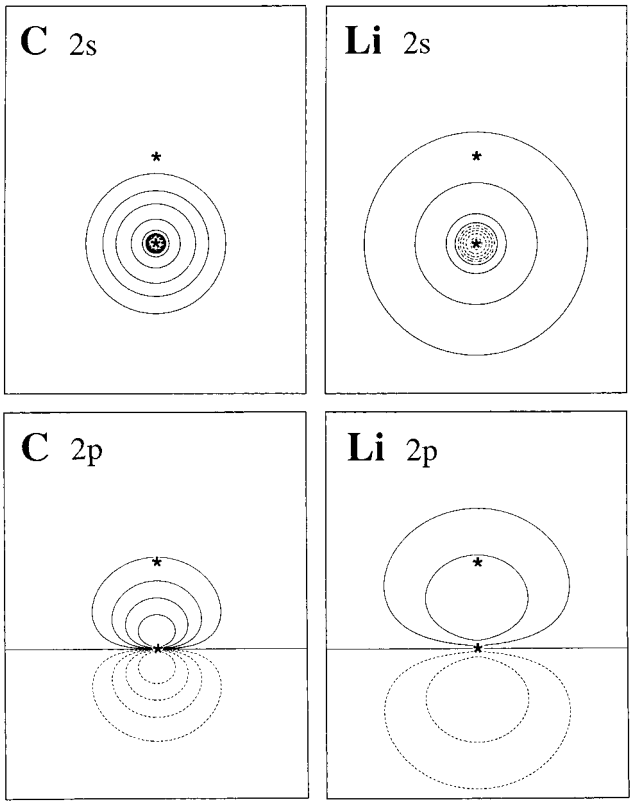

Figure 5. Contour plots of Li and C 2s and 2p AOs. Asterisks show the Li−Li separation in $(Li^{\bullet})_2$. Scan values: 0.0, ±0.02, ±0.05, ±0.10, ±0.2, ±0.5. Radial nodes are dash−dotted.

preparation energy of 14.1 kcal/mol due to the strong Pauli repulsion between the two 2sα electrons. This Pauli repulsion however also causes an effective s → p promotion by which it is partly relieved (Figure 4).

The electronic structure of $(Li^{\bullet})_2$ (Figure 4) differs from that of the late first-row diatomics[16] due to the very diffuse nature of the lithium orbitals (Figure 5). The large $\langle 2s|2s\rangle$ overlap of 0.69 (Table 2) and a strong 2s ± 2s level splitting cause the antibonding 2s − 2s combination to rise above the 2p combinations, whereas the exceptionally small $\langle 2p_z|2p_z\rangle$ overlap of 0.01 yields weakly split $2p_z \pm 2p_z$ levels which are in between those of the stronger interacting $2p_\pi \pm 2p_\pi$ combinations ($\langle 2p_\pi|2p_\pi\rangle = 0.58$, Table 2). As a result, $SOMO_{low}$ and $SOMO_{high}$ are given by 2s + 2s ($1\sigma_g$) and one of the $2p_\pi + 2p_\pi$ combinations ($1\pi_{u,x}$ in our calculations). The reason for the poor $\langle 2p_z|2p_z\rangle$ and the large $\langle 2p_\pi|2p_\pi\rangle$ and $\langle 2s|2s\rangle$ overlaps is the very diffuse character of lithium 2s and 2p AOs (compare with carbon 2s and 2p in Figure 5) and a relatively short Li−Li distance of 2.147 Å (compare with 2.78 Å in ground state Li_2). Due to this, the $2p_z$ AOs in $(Li^{\bullet})_2$ penetrate into the nodal surface of each other, which leads to cancellation of overlap. The extended nature of the lithium AOs is however favorable for the $\langle 2s|2s\rangle$ and $\langle 2p_\pi|2p_\pi\rangle$ overlaps. Note that the sizable mutual stabilization that the lithium 2p orbitals experience in the metal cluster puts them effectively into the role of "normal" valence orbitals.

Two orbital interactions comprise the carbon−lithium bonding in $(CH_3Li)_2$: (1) the $SOMO_{low}$ interaction $3a_g \pm 1\sigma_g$; (2) the $SOMO_{high}$ interaction $3b_u \pm 1\pi_{u,x}$ (Figure 3). The first interaction results in a less polar, yet stronger electron pair bond, compared to monomeric CH_3Li; the dimethyl $3a_g$ population $P(SOMO_{low})$ is 1.36 e, while the interaction energy is −92.8 kcal/mol. The explanation is simple: the $3a_g - 1\sigma_g$ energy difference is lower, due to the relatively low energy of the $(Li^{\bullet})_2$ $1\sigma_g$ (−4.2 eV), and the $3a_g - 1\sigma_g$ overlap is larger, 0.47.

The $SOMO_{high}$ interaction results in a highly polar electron pair bond. The $3b_u - 1\pi_{u,x}$ overlap is low, only 0.26 (Table 2), since the relative orientation of the fragment orbitals is less favorable than for the $SOMO_{low}$ combination, where the maximum amplitude regions coincide. However, the strong charge donation from the high energy $(Li^{\bullet})_2$ $1\pi_{u,x}$ (−2.3 eV) to the $(CH_3^{\bullet})_2$ $3b_u$ significantly increases the population of the dimethyl $3b_u$ ($P(SOMO_{high}) = 1.52$ e). The stabilization resulting from this charge donation is reflected in the energy contribution ΔE_{high} of −138.0 kcal/mol. The residual orbital interaction energy (ΔE_{rest} = −3.2 kcal/mol) contains "agostic" interactions between lower $(CH_3^{\bullet})_2$ fragment orbitals (derived from the C−H bonding methyl $1e_1$ orbitals) and $(Li^{\bullet})_2$.

The orbital interactions ΔE_{oi} (−234.0 kcal/mol) are opposed by a steric repulsion $\Delta E_{Pauli} + \Delta E_{elst} = 58.0$ kcal/mol (due to valence−valence as well as core−valence overlap) and a preparation energy $\Delta E_{prep} = 43.3$ kcal/mol, leading to the overall bond energy ΔE = −132.7 kcal/mol (i.e. −66.4 kcal/mol per methyllithium).

Methyllithium Tetramer. Finally, we discuss the carbon−lithium bond in $(CH_3-Li)_4$. The corresponding $(CH_3^{\bullet})_4$ and $(Li^{\bullet})_4$ fragments have quintet electronic structures with one electron in a C−C (or Li−Li) bonding ($SOMO_{low}$) and three electrons in a set of triply degenerate C−C (or Li−Li) antibonding orbitals ($SOMO_{high}$, Figure 6). The preparation energy of the $(CH_3^{\bullet})_4$ "cage" (66.7 kcal/mol) is again mainly due to methyl

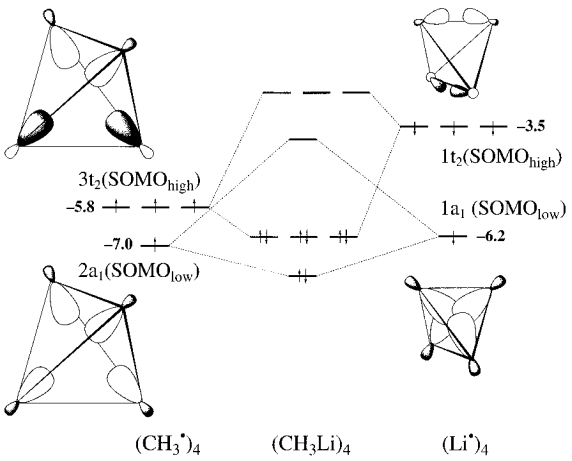

Figure 6. Orbital interaction diagram for $(CH_3Li)_4$.

pyramidalization. The energy gap of 1.2 eV between $SOMO_{low}$ ($2a_1$, C−C bonding) and $SOMO_{high}$ ($3t_2$, C−C antibonding) is slightly larger than the corresponding gap in $(CH_3^{\bullet})_2$, due to the participation of four instead of only two $CH_3^{\bullet}$ $2a_1$ orbitals (Figure 6).

Interestingly, the formation of the tetrahedral quintet $(Li^{\bullet})_4$ is slightly exothermic (−3.3 kcal/mol) and not endothermic as might be expected for four strongly overlapping ($\langle 2s|2s\rangle = 0.65$) same-spin 2s orbitals. The reason is a significant stabilization of the 2p orbitals in the lithium cluster and a strong 2s−2p rehybridization (effectively again s → p transfer), which heavily stabilizes both $1a_1$ and $1t_2$ (compare $(Li^{\bullet})_2$ in Figure 3). Thus, the low-energy lithium 2p orbitals may again be viewed as "normal" valence orbitals.

Carbon−lithium bonding in $(CH_3Li)_4$ is again provided by two distinct orbital interactions: (1) the $SOMO_{low}$ interaction $2a_1 \pm 1a_1$; (2) the triply degenerate $SOMO_{high}$ interaction $3t_2 \pm 1t_2$ (Figure 6). The former gives an *essentially covalent* electron pair bond of −85.8 kcal/mol; the $SOMO_{low}$ populations are 1.02 and 0.91 e for the tetramethyl ($2a_1$) and the tetralithium ($1a_1$) fragment, respectively (Table 2)! The extremely low polarity of this C−Li electron pair bond is due to the very low energy of the $(Li^{\bullet})_4$ $1a_1$: 3 eV below lithium 2s and only 0.8 eV above $(CH_3^{\bullet})_4$ $2a_1$ (Figure 6). The absence of charge transfer in this bond is held responsible for the slightly weaker ΔE_{low} compared to $(CH_3Li)_2$, in spite of the larger $2a_1-1a_1$ overlap of 0.55 (Table 2).

The triply degenerate $SOMO_{high}$ interactions provide a strong bond of −387.0 kcal/mol, i.e. −129.0 kcal/mol per electron, because of the stabilization associated with the sizable charge donation from the higher energy $(Li^{\bullet})_4$ $1t_2$ (−3.5 eV) to the $(CH_3^{\bullet})_4$ $3t_2$ which overrules the unfavorable effect of the relatively small overlap of 0.29 (Table 2). This component of the C−Li bond is highly polar and significantly increases the tetramethyl $3t_2$ population ($P(SOMO_{high}) = 1.43$ e), although less so than in $(CH_3Li)_2$. The "agostic" interactions between C−H bonds and lithium (contained in $\Delta E_{rest} = -18.7$ kcal/mol) are significantly larger than in the monomer and dimer (see also NBO analysis, section 3A) and lead to a shortening of the Li−H distance, because the C−H and C−Li bonds are eclipsed. Note, that the specific depopulation of the (weakly) Li−Li antibonding $1t_2$ orbitals (together with the remaining population of the Li−Li bonding $1a_1$) improves the coherence within the positively charged $(Li^{\bullet})_4$ cluster.

The orbital interactions ΔE_{oi} (−491.5 kcal/mol) are opposed by steric repulsion $\Delta E_{Pauli} + \Delta E_{elst} = 119.5$ kcal/mol (due to both valence−valence and core−valence overlap) and a preparation energy $\Delta E_{prep} = 63.4$ kcal/mol, leading to the overall bond energy $\Delta E = -308.6$ kcal/mol (i.e. −77.2 kcal/mol per methyllithium).

4. Conclusions

This investigation highlights the important role of a covalent component in the polar C−Li bond, especially in the methyllithium tetramer. This may help to explain experimental observations such as the large C−Li NMR coupling constants.[9]

The carbon−lithium bond in methyllithium oligomers may well be envisaged as an electron pair bond, although a strongly polar one, as follows from our NL-SCF/TZ2P calculations. In the dimer and tetramer, it is composed of two distinct orbital interactions: (1) a relatively covalent electron pair bond between C−C and Li−Li bonding $(CH_3^{\bullet})_n$ and $(Li^{\bullet})_n$ fragment orbitals; (2) a strongly polar interaction between the corresponding C−C and Li−Li antibonding (in $(Li^{\bullet})_2$ π bonding) fragment orbitals.

In $(CH_3Li)_4$, the first component (in A_1 symmetry) even provides an *essentially covalent* C−Li electron pair bond. The second component (in T_2 symmetry) is responsible for the large charge donation from lithium to methyl. This charge donation stabilizes the Li−Li bonding within the lithium cluster because the Li−Li *antibonding* $(Li^{\bullet})_4$ $1t_2$ orbitals are depopulated whereas the population of the Li−Li *bonding* $(Li^{\bullet})_4$ $1a_1$ is more or less conserved.

The lithium 2p AOs should be viewed as valence orbitals and not as superposition functions. Their significant role evolves from their sizable participation in the C−Li bond and from the significant lithium 2s−2p rehybridization in the singly occupied $(Li^{\bullet})_2$ and $(Li^{\bullet})_4$ frontier orbitals. One of the SOMOs in the lithium dimer is in fact a 100% 2p based orbital (i.e. $2p_{\pi,x} + 2p_{\pi,x}$; see Figures 3 and 4). This point is underlined by the fact that the MP4SDQ oligomerization energies are lowered by up to 20% when Li 2p functions are omitted from the 6-31+G* basis set.

Although we have emphasized the important role of covalent contributions to the C−Li bond, we certainly do not wish to imply a purely covalent picture. In fact, our results emphasize the *dual character* of the C−Li bond. We conclude that the appearance of the covalent (gas-phase dissociation, NMR) or ionic aspect (metalation reactions,[25] charge distribution) strongly depends on the physical and chemical context.[1−9,25]

Acknowledgment. We dedicate this paper to Prof. Paul von Ragué Schleyer, in honor of his achievements in computational and experimental organolithium chemistry. The present investigation was greatly inspired by his pioneering work in this area. Support by the Deutsche Forschungsgemeinschaft (DFG) and the Netherlands Organization for Scientific Research (NCF/NWO) is gratefully acknowledged. F.M.B. thanks the DFG for a postdoctoral fellowship.

OM950966X

(25) Elschenbroich, Ch.; Salzer, A. *Organometallics. A Concise Introduction*, 2nd ed.; VCH: Weinheim, Germany, 1992.